

Accepted Manuscript

Phenylboronic acid-diol crosslinked 6-O-vinylazelo-yl-d-galactose nanocarriers for insulin delivery

Jun-zi Wu, David H. Bremner, He-yu Li, Shi-Wei Niu, Shu-De Li, Li-Min Zhu



PII: S0928-4931(16)32829-6

DOI: doi: [10.1016/j.msec.2017.03.139](https://doi.org/10.1016/j.msec.2017.03.139)

Reference: MSC 7650

To appear in: *Materials Science & Engineering C*

Received date: 27 December 2016

Revised date: 9 March 2017

Accepted date: 13 March 2017

Please cite this article as: Jun-zi Wu, David H. Bremner, He-yu Li, Shi-Wei Niu, Shu-De Li, Li-Min Zhu , Phenylboronic acid-diol crosslinked 6-O-vinylazelo-yl-d-galactose nanocarriers for insulin delivery. The address for the corresponding author was captured as affiliation for all authors. Please check if appropriate. Msc(2017), doi: [10.1016/j.msec.2017.03.139](https://doi.org/10.1016/j.msec.2017.03.139)

This is a PDF file of an unedited manuscript that has been accepted for publication. As a service to our customers we are providing this early version of the manuscript. The manuscript will undergo copyediting, typesetting, and review of the resulting proof before it is published in its final form. Please note that during the production process errors may be discovered which could affect the content, and all legal disclaimers that apply to the journal pertain.

Phenylboronic acid-diol crosslinked 6-O-vinylazeloyle -D-galactose nanocarriers for insulin delivery

Jun-zi Wu ^a, David H Bremner ^b, He-yu Li ^a, Shi-Wei Niu ^a, Shu-De Li ^c, Li-Min Zhu ^{a*}

^a College of Chemistry, Chemical Engineering and Biotechnology, Donghua University, Shanghai
201620, P.R. China

^b School of Science, Engineering and Technology, Kydd Building, Abertay University, Dundee
DD1 1HG, Scotland, UK

^c School of Basic Medical Sciences, Kunming Medical University, Kunming, 650228, P.R. China

***Corresponding author:**

Prof. L.M. Zhu

College of Chemistry, Chemical Engineering and Biotechnology, Donghua University,

2999 North Renmin Road, Songjiang District,

Shanghai 201620, China, Tel: +86-21-67792748, Fax: +86-21-62372655,

E-mail: lzhu@dhu.edu.cn

Revise to *Material science and engineering C*

ABSTRACT

A new block polymer named poly 3-acrylamidophenylboronic acid-b-6-O-vinylazeloyle-D-galactose (p(AAPBA-b-OVZG)) was prepared using 3-acrylamidophenylboronic acid (AAPBA) and 6-O-vinylazeloyle-D-galactose (OVZG) via a two-step procedure involving S-1-dodecyl-S-(α' , α' -dimethyl- α'' -acetic acid) trithiocarbonate (DDATC) as chain transfer agent, 2,2-azobisisobutyronitrile (AIBN) as initiator and dimethyl formamide (DMF) as solvent. The structures of the polymer were examined by Fourier transform infrared spectroscopy (FT-IR) and $^1\text{H-NMR}$ and the thermal stability was determined by thermal gravimetric analysis (TG/DTG). Transmission electron microscopy (TEM) and dynamic light scattering (DLS) were utilized to evaluate the morphology and properties of the p(AAPBA-b-OVZG) nanoparticles. The cell toxicity, animal toxicity and therapeutic efficacy were also investigated. The results indicate the p(AAPBA-b-OVZG) was successfully synthesized and had excellent thermal stability. Moreover, the p(AAPBA-b-OVZG) nanoparticles were submicron in size and glucose-sensitive in phosphate-buffered saline (PBS). In addition, insulin as a model drug had a high encapsulation efficiency and loading capacity and the release of insulin was increased at higher glucose levels. Furthermore, the nanoparticles showed a low-toxicity in cell and animal studies and they were effective at decreasing blood glucose levels of mice over 96h. These p(AAPBA-b-OVZG) nanoparticles show promise for applications in diabetes treatment using insulin or other hypoglycemic proteins.

Keywords: 3-Acrylamidophenylboronic Acid (AAPBA), 6-O-vinylazeloyle-D-galactose (OVZG), Nanoparticles (NPs), Glucose-Sensitive, Insulin Delivery.

1. Introduction

Epidemiological investigations have shown that in 2011 there were about 366 million diabetics worldwide and about 1.3 million diabetes patients died which is twice the figure seen in 1990 [1]. Moreover, the incidences of diabetes and mortality rates have continued to increase over the last 5 years [2-4]. Thus, there is little doubt that diabetes has become a serious disease that affects many, otherwise healthy people, and new methodology of controlling blood sugar levels is desperately needed for diabetes patients [5]. Generally speaking, there are three methodologies used in the treatment of diabetes: primary prevention measures; healthy lifestyle changes; and long term management [6]. Primary prevention measures and healthy lifestyle changes usually involve increasing physical exercise and diet control. Long term management of diabetes involves intensive glycemic control utilizing drugs such as epaglinide, insulin, liraglutide, metformin, acarbose, or rosiglitazone hydrochloride [7-9] although insulin is still the most effective and cheapest drug. However patients have different body weights and variable glucose levels, so the required dose of insulin needed to return their glucose levels to normal can vary widely. Also there is the issue of injecting too much insulin resulting in hypoglycemia or too little leading to rapid heartbeat and polyuria [10-11]. Consequently the development of a smart response system is highly desirable.

In recent years, functional biological materials have been studied extensively in drug delivery systems, due to their low price and excellent biocompatibility and they have shown great promise [12-14]. Glucose-responsive delivery systems based on biological materials have rarely been reported [15-18]. Those that have been described are usually based on phenylboronic acid (PBA) and/or derivatives of phenylboronic acid. For example, Wang et al. [19] used a two-step template

polymerization to prepare new temperature- and glucose-responsive nanogels based on poly(N-isopropyl-acrylamide) and poly-(N-phenylboronic acid-acrylamide). They found that these nanogels had interpenetrating polymer networks and good glucose response. Also Sun et al. [20] prepared poly(N-isopropylacrylamide-co-3-acrylamidophenylboronic acid -co-dextran-maleic acid) coated silica nanoparticles via radical polymerization and found the cumulative release of insulin in vitro was dependent on glucose concentration. In addition, previously, we reported [21] the synthesis of a new temperature-sensitive copolymer named p(NVCL-co-AAPBA) from N-vinylcaprolactam (NVCL) and 3-acrylamido phenylboronic acid (AAPBA) and found that it had excellent glucose-response. However, all the previous work [19-21] resulted in compounds having a short duration of activity (8-48h) due to degradation of the nanoparticles based on phenylboronic acid and consequently required frequent injections which brings new problems, so it is imperative to develop products that release insulin when required.

Glycopolymers are a type of functional polymeric material synthesized using different biological and chemical reactions, which maintain the special properties of sugars, but also have some new functionalities such as good hydrophilicity, biocompatibility and biodegradability [22]. Guo et al. [23] described the synthesis of a block and random co-polymer based on the PBA and glycopolymers using the phenylboronic acid-based glycopolymer poly(3-acrylamido-phenylboronic acid-b-2-acrylamido glucopyranose) p(AAPBA-b-AGA) and found that the nanoparticles had a high glucose-response but had the disadvantage of having a cumulative release time of only 16 h. Galactose and glucose can also react with diolefinic acid to produce compounds containing a single olefinic acid which can be formed into glycopolymers by polymerization. Thus, Kan Sun et al. [24] synthesized poly(N-isopropylacrylamide-co-6-O-vinyladipoyl -D-glucose)-b

-poly(N-isopropylacrylamide) and found that the pendant glucose moieties had obvious interaction with lectin and concanavalin A (Con A). Due to the compound containing fructose, galactose and glucose it is easy to form a glycopolymers [25], so it is to be expected that AAPBA will react with glycopolymers containing fructose, galactose or glucose to form a new copolymer which may be responsive to glucose levels in blood, and further increase the cumulative release times.

In this work, a new glycopolymer, 6-O-vinylazeloil-D-galactose (OVZG) was first synthesized and this was then combined with PBA to give a glucose sensitive polymer poly 6-O-vinylazeloil-D-galactose-b-3-acrylamidophenylboronic acid (p(AAPBA-b-OVZG)). Thereafter, *in vitro* studies on the insulin loading, encapsulation and release from the nanoparticles were performed and their toxicology was examined both *in vitro* and *in vivo*. Finally, the therapeutic effects of the formulations were assessed using a mouse model of diabetes. We believe that the stimuli-responsive systems described in this work may have great potential for the development of advanced insulin delivery systems.

2. Materials and Methods

2.1. Materials

3-Acrylamidophenylboronic acid (AAPBA) was purchased from the Beijing Pure Chem. Co., Ltd. (Beijing, PR China) and alkaline protease (from *Bacillus subtilis*, 100 U per mg) was obtained from the Wuxi Xue Mei Co. Ltd. (EC 3.4.21.14, Wuxi, PR China). Azelaic acid was purchased from the Sinopharm Chemical Reagent Co. (Shanghai, PR China); S-1-dodecyl-S-(α' , α' -dimethyl- α'' -acetic acid) trithiocarbonate (DDATC) was obtained from Sigma-Aldrich Trading Co., Ltd.; 2-[4-(2-Hydroxyethyl)-1-piperazinyl] ethanesulfonic acid (HEPES) was procured from the Nanjing Robiot Co. (Nanjing, PR China). Dimethylformamide (DMF), dimethyl sulfoxide

(DMSO) and 2,2-azobisisobutyronitrile (AIBN) was purchased from the Sinopharm Chemical Reagent Co., Ltd. (Shanghai, PR China). All solvents used in this work were analytical grade.

2.2. Synthesis of p(AAPBA-b -OVZG).

2.2. 1 Synthesis of 9-O-viny azelaicoyl-D-galactose (OVZG).

OVZG was synthesized as previously reported [26] via the chemoenzymatic route.

2.2.2. Synthesis of poly(3-acrylamidophenylboronic acid) (pAAPBA).

The synthesis of pAAPBA was based on a previous method [27] using AAPBA (300 mg), DDATC (3 mg), AIBN (0.3 mg) and N,N-dimethylformamide (DMF; 1 mL) as solvent. The reaction mixture was sealed in a reaction vessel (50 mL) and was subjected to three freeze–thaw cycles under vacuum. The reaction vessel was then placed in a preheated oil bath (70 °C) for 8 hours and then cooled in ice water for 5 min. The resultant polymer was precipitated by pouring the solution into diethyl ether, filtered and washed with acetone and dried under vacuum.

2.2.3. Synthesis of p(AAPBA-b-OVZG).

p(AAPBA-b-OVZG) was prepared via RAFT copolymerization, using OVZG as a monomer, the homopolymer pAAPBA as a macro RAFT agent, AIBN as the initiator, and DMF as the solvent. The reaction mixture was sealed in a reaction vessel (50 mL) and was subjected to three freeze–thaw cycles under vacuum. And then the same procedure as described above (2.2.2. Synthesis of poly(3-acrylamidophenylboronic acid) (pAAPBA)) was followed. By changing the ratio of pAAPBA to OVZG, five different glycopolymers were prepared and named as p(AAPBA-b-OVZG)1, p(AAPBA-b -OVZG)2, p(AAPBA-b-OVZG)3, p(AAPBA-b-OVZG)4 and p(AAPBA-b-OVZG)5.

2.3. Characterization of the polymers

The polymers were characterized using Fourier transform infrared spectroscopy (FT-IR), thermogravimetric analysis, $^1\text{H-NMR}$ and Gel Permeation Chromatography (GPC). As previously reported [24], FT-IR spectra were recorded on a Fourier Transform Infrared Spectrometer (FTS-6000, Bio-Rad Co.) at a resolution of 2 cm^{-1} , using a KBr solid solution. The thermogravimetric analysis of the copolymer was conducted with a thermogravimetric analyzer (TGA, STA409PC), where the sample (3-5 mg) was heated at a rate of $10\text{ }^\circ\text{C}/\text{min}$ in a nitrogen atmosphere. $^1\text{H-NMR}$ spectra were obtained using purified polymer samples (3-5mg) in $\text{D}_2\text{O}+\text{NaOD}$ (1mL, pH=9.0) with a Bruker DRX 400 MHz spectrometer (Bruker, Rheinstetten, Germany). The molecular weights (M_w and M_n) and molecular weight distributions of the polymers were determined by GPC measurements on a Waters LS system.

2.4 Preparation of Nanoparticles (NPs)

P(AAPBA-b-OVZG) NPs were prepared according to a previously reported method [28] using p(AAPBA-b-OVZG) (10 mg) dissolved into dimethyl sulfoxide (DMSO) and water (2 mL; 1:1 v/v). This solution was added dropwise into ultra-pure water (20 mL) with stirring (300r/min). After 3h, the suspension was centrifuged (10min; 12000r/min), the supernatant discarded and then ultra-pure water (20mL) was added. The resulting suspension was transferred to a dialysis tube (MWCO 8000) and dialyzed against water for 72 h with the water being replaced every 4 h in order to remove the organic solvent. The suspension was then vacuum freeze dried to give pure NPs.

In order to prepare the insulin-loaded NPs, insulin (500 μg) was dissolved in a sodium acetate solution (20 mL; 0.5%) and the solution of the NPs was added dropwise as described above.

After dialysis for 72 h, the suspension of insulin-loaded NPs was centrifuged at 12000 rpm for 20

min and the amount of free insulin in the supernatant was measured using the Bradford method with a UV spectrometer (Shimadzu UV-2550) at 595 nm. The insulin Encapsulation Efficiency (EE) and Loading Capacity (LC) were calculated according to the following equations:

$$EE\% = (\text{total insulin-free insulin})/\text{total insulin} \times 100$$

$$LC\% = (\text{total insulin-free insulin})/\text{NPs weight} \times 100$$

2.5 Transmission Electron Microscopy (TEM).

The TEM micrographs were obtained using a transmission electron microscope (JEM-2100, JEOL, Japan). The samples were prepared by placing a drop of the p(AAPBA-b-OVZG) ultra-pure water solution (0.3 mg/mL) onto a copper grid and drying at 36 °C.

2.6 Reversible pH and glucose sensitivity of the NPs

The pH and glucose sensitivity were determined by using the blank p(AAPBA-b-OVZG) NPs. The pH sensitivity was measured by suspending the pure NPs (10 mg) in ultra-pure water (25 mL) at pH 5.0, 5.5, 6.0, 6.5, 7.0, 7.5, 8.0, 8.5 and 9.0 for 0.5 h. The size of the NPs was measured by dynamic light scattering (DLS, Malvern Zetasizer Nano S apparatus equipped with a 4.0 mV laser operating at $\lambda=636$ nm) at 37 °C.

Glucose sensitivity was determined by using the blank NPs (10mg) with 0, 1.0, 2.0, and 3.0 mg/mL glucose in PBS (25mL) for 0, 10, 20, 30, 40, 50 and 60 min, and then the size of the NPs was measured by DLS at 37 °C.

2.7 *In vitro* release behavior

In order to determine the *in vitro* release, the different insulin-loaded NPs (5 mg) were mixed with PBS (20 mL; 0.1 M, pH=7.4) containing different glucose concentrations (0, 1, 2 and 3 mg/mL) and shaken (100r/min) at 37 °C. After a predetermined time, an aliquot of supernatant (1 mL) was

removed and fresh buffer solution was added. The amount of free insulin was monitored by UV spectrophotometry with each sample being analyzed in triplicate and the results reported as the mean \pm standard deviation ($n=3$).

2.8 Toxicity

2.8.1 Cell viability study and MTT assays.

The MTT assay was used to evaluate the cell viability of the p(AAPBA-b-OVZG) NPs with NIH 3T3 cells cultured in a modified Dulbecco Eagle's medium (DMEM, Gibco) in a humidified atmosphere of 5 % CO₂. The cells were seeded into 96-well plates at a density of 1×10^4 cells per well and suspensions of p(AAPBA-b-OVZG) NPs (100 mL) with concentrations ranging from 20 to 120 mg/mL were added and incubated for 24 h. Then MTT solution in PBS buffer (20 μ L; 5 mg/mL) was added to each well and then removed four hours later. The samples in the wells were allowed to dry naturally for 4h, DMSO (200 μ L) was added to dissolve the formed crystals and the optical density of the solution was measured at 570 nm using a microplate reader (Thermo Multiskan MK3, Thermo Scientific Company, Waltham, UK). The NIH 3T3 cells without any treatment were used as the control.

2.8.2 Acute animal toxicity

A total of 24 Kunming mice (12 males and 12 females; 19-23 g) were obtained from the Animal Center of Kunming Medical University (Kunming, China). All the mice were given 2 weeks adaptive feeding, and then were randomly divided into the control group and the experimental groups (low, middle and high doses, $n=6$). After 2 weeks, the control group was injected with saline solution (1 mL/d) intraperitoneally, and the low, middle and high dose group were given p(AAPBA-b-OVZG)₄ NPs (100 mg/kg/d, 200 mg/kg/d and 400 mg/kg/d respectively) using the

same method. After 7 days, all the mice were sacrificed and their livers, kidneys, spleens, hearts and lungs were collected for Hematoxylin and Eosin (HE) staining in order to detect if any visceral damage had occurred.

2.8.3 Chronic toxicological experiments

A total of 24 Kunming mice (12 males and 12 females; 19-23 g) were divided into the control group ($n=6$) and the experimental groups (10, 20 and 40 mg/kg/d-dose) randomly. The experimental mice received intraperitoneal injections with the appropriate doses of p(AAPBA-b-OVZG)₄ NPs and the control group received injections of saline solution (1 mL/kg/d). After 60 days, the mice were sacrificed, their blood was collected and the concentrations of Red Blood Cells (RBC), White Blood Cells (WBC), Platelet, Hemoglobin, Serum protein, Serum creatinine, Hematocrit, Serum glutathione, Total cholesterol, Glucose, Uric acid, Aspartate aminoTransferase (AST) and Glutamine Transaminase (ALT) were determined using an automated Olympus AU5400 biochemistry analyzer (Olympus, Tokyo, Japan).

2.9 *In vivo* hypoglycemic experiments

All the diabetes mellitus mice (fasting blood glucose levels >15.6 mmol/L, $n=18$) were provided kindly by the College of Basic Medical Sciences of Kunming Medical University and were randomly allocated into a high fat group ($n=6$), an insulin injection group ($n=6$) and a p(AAPBA-b-OVZG)₄ group ($n=6$) and six other healthy mice were chosen as a control group (CG). The mice in the p(AAPBA-b-OVZG) group received insulin-loaded p(AAPBA-b-OVZG)₄ NPs (1 mL/kg, contained 1.0 mg insulin, the solvent was 0.6% normal saline) injections, those in the insulin injection group received insulin injection (1 mL/kg, contained 0.16 mg insulin, the solvent was 0.6% sodium acetate solution) and the remaining mice in the high fat group and in the

control group were given distilled water (0.5 mL/kg) injection every day. The blood of mice was collected from tail veins and the blood glucose levels were measured by a Blood Glucose Meter ((GT-1640); Jiangxi Jingdou Co., Ltd. Nanchang, PR China). In addition, the blood was centrifuged (3000 rpm, 10 min), the supernatant collected and the insulin level was determined at 0h, 1h, 2h, 3h, 4h, 5h, 6h, 12h, 24h, 36h, 48h, 60h, 72h, 84h, 96h, 108h and 120h using an appropriate insulin ELISA kit (China Institute of Atomic Energy, China). All the animal experimental operations were in line with the Guide for the Care and Use of Laboratory Animals published by the US National Institutes of Health (NIH Publication No. 8523, revised 1985) and all the experiments were approved by the Animal Care and Use Committee of Kunming Medical University (certificate number: KMMU 2014002).

3 Results

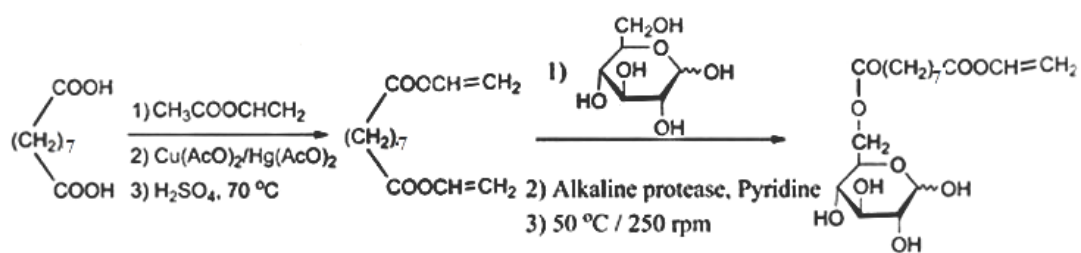
3.1 Characterization of the Block and Random Copolymers.

The p(AAPBA-b-OVZG) glycopolymers were synthesized in good yields (Table 1) via a sequential RAFT polymerization process (Scheme 1 and Scheme 2).

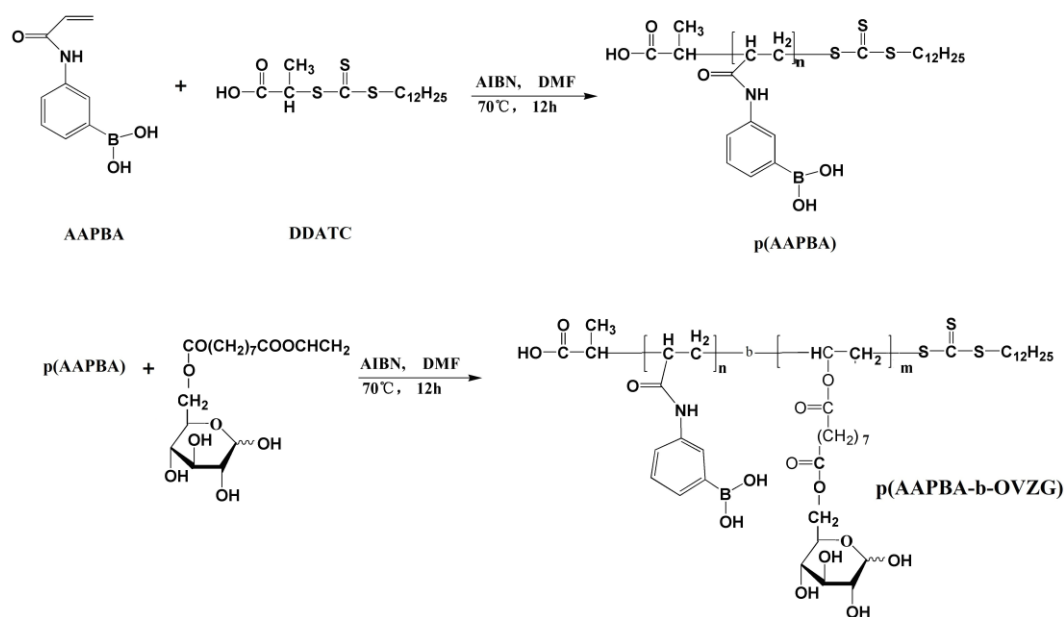
Tab.1. Constitution and yield of the copolymers

Sample	Monomer (mol/mol)	yield (%)
p(AAPBA-b-OVZG)1	OVZG/AAPBA =100: 10	65.43
p(AAPBA-b-OVZG)2	OVZG/AAPBA =100: 20	72.62
p(AAPBA-b-OVZG)3	OVZG/AAPBA =100: 50	69.37
p(AAPBA-b-OVZG)4	OVZG/AAPBA =100: 100	70.56
p(AAPBA-b-OVZG)5	OVZG/AAPBA =100: 200	74.29

Note: yield was calculated via weight method.



Scheme 1. The synthesis of OVZG by controllable chemo enzymatic reaction.



Scheme 2. The synthesis of p(OVZG-b-AAPBA) by RAFT polymerization.

The FT-IR spectra of AAPBA, OVZG, p(AAPBA) and p(AAPBA-b-OVZG)₄ are shown in Fig.1. AAPBA displays four characteristic absorption bands: C=O str. at 1660 cm⁻¹, C=C str. at 1620 cm⁻¹, O-B-O at 1352 cm⁻¹ and B-O at 1014 cm⁻¹. The benzene ring skeleton is present between 1555-1610 cm⁻¹ and the meta-substituted benzene absorptions are at 698 cm⁻¹ and 791 cm⁻¹. OVZG shows C=O str. at 1740 cm⁻¹, C=C str. at 1650 cm⁻¹, -NH str. at 1490 cm⁻¹ and the absorption at 1920 cm⁻¹ is the overtone 960 cm⁻¹. In p(AAPBA) and p(AAPBA-b-OVZG)₄, the absorption due to C=C disappears indicating that successful polymerization had occurred and in the FT-IR spectrum of p(AAPBA-b-OVZG)₄ there exists B-O str. at 996 cm⁻¹, which proves AAPBA had been incorporated into the polymer.

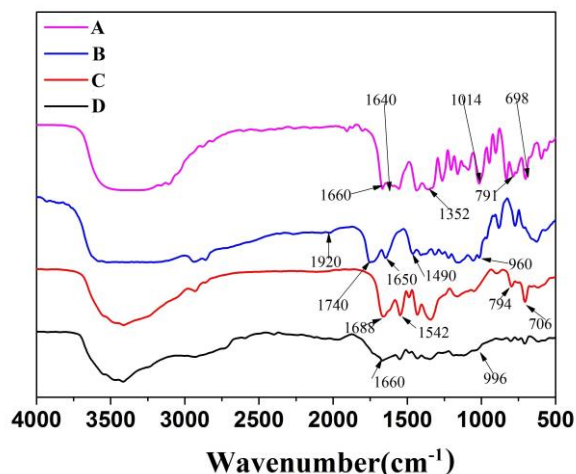


Fig.1. FT-IR spectra of (A) OVZG, (B) AAPBA, (C) pAAPBA and (D) p(AAPBA-b-OVZG)4

Figure 2 shows the $^1\text{H-NMR}$ spectra of OVZG, AAPBA, p(AAPBA) and p(AAPBA-b-OVZG)4.

The spectrum of OVZG (Figure 2A) ($\text{D}_2\text{O} + \text{DMSO-d}_6$) δ : 6.95(1H, 3-H), 6.35(1H, 8-H), 4.75(2H, 1-H), 4.65 (1H, 2-H), 4.55(2H, 7-H), 4.15 (1H, 6-H), 3.95 (1H, 5-H) and 3.45 (1H, 4-H). AAPBA (Figure 2B) shows the following assignments: $^1\text{H NMR}$ ($\text{NaOD} + \text{D}_2\text{O}$; pH = 9.5): δ : 10.09 (1H, 4-H), 8.10-7.25 (the H of benzene ring), 6.47 (1H, 2-H), 6.20 (1H, 3-H) and 5.75 (2H, 1-H). p(AAPBA) (Figure 2C) ($\text{NaOD} + \text{D}_2\text{O}$; pH = 9.5) δ : 8.40-6.33 (the H of benzene ring), 2.95 (2H, 10-H), 2.14 (1H, 4-H), 1.75 (1H, 9-H), 0.50-1.25 and 2.33 (the $\text{C}_{12}\text{H}_{25}$, 1-H, 2-H and 3-H) and the p(AAPBA-b-OVZG)4 (Figure 2D) ($\text{NaOD} + \text{D}_2\text{O}$; pH = 9.5) δ : 8.10-7.15 (the H of benzene ring), 5.05 (1H, 4-H), 4.05(1H, 5-H), 3.45-3.75(the H of $(\text{CH}_2)_7$, 3-H), 3.25 (4H, 2-H), 2.80(1H, 7-H), 2.65(1H, 1-H), 1.65(2H, 8-H) and 1.75 (2H, 6-H). Compared with the spectra of the monomers AAPBA and OVZG, it is obvious that the peaks of ethylene in p(AAPBA) and p(AAPBA-b-OVZG)4 have disappeared and the peaks of these protons can be assigned in the structure of p(AAPBA-b-OVZG)4. The H of benzene ring in p(AAPBA) and p(AAPBA-b-OVZG)4 have slightly different chemical shifts compared to a previous report [23],

which may be due to the different solvent used

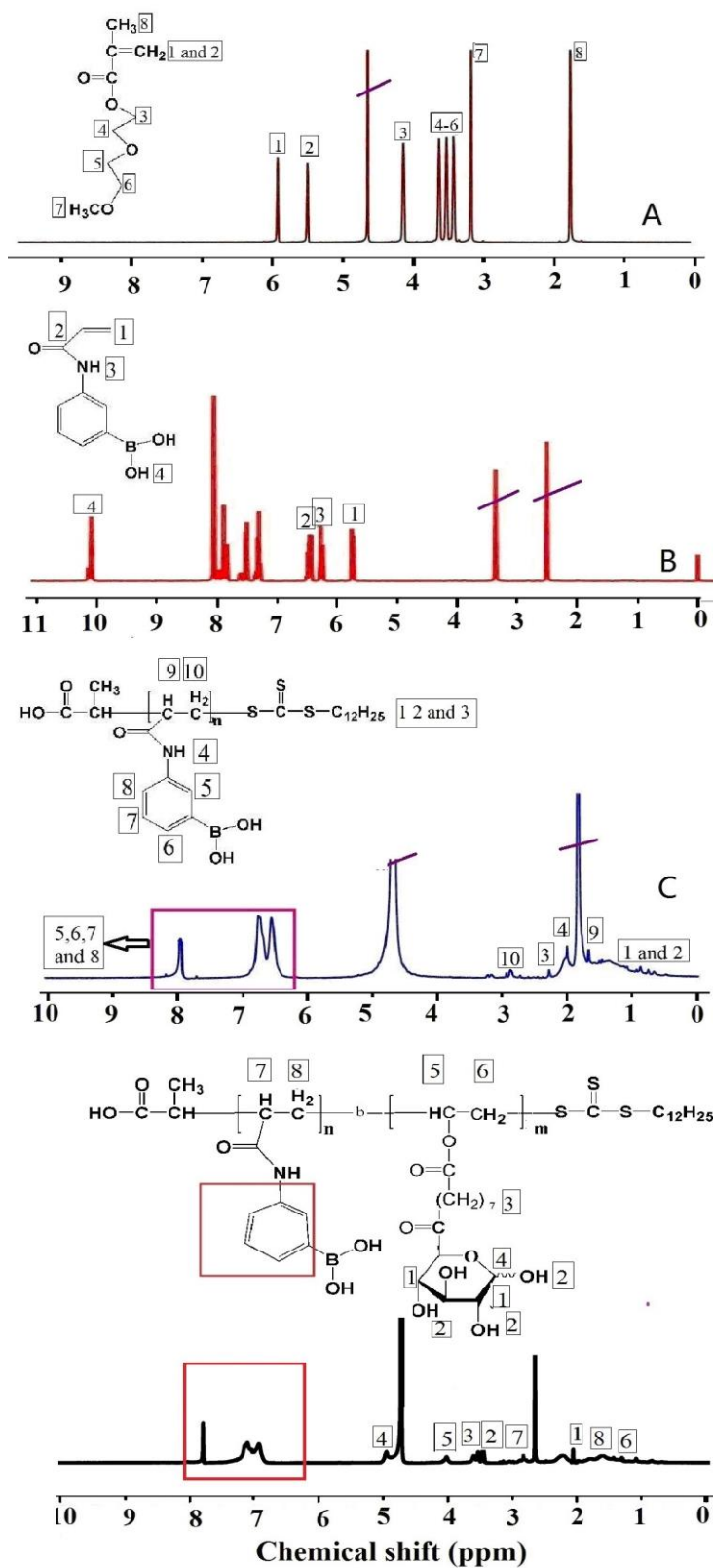


Fig.2. ^1H NMR spectra of (A) OVZG, (B) AAPBA, (C) pAAPBA and (D) p(AAPBA-b-OVZG)4.

Figure 3 shows the thermogravimetric (TG) and derivative thermogravimetric (DTG) curves for pAAPBA and p(AAPBA-b-OVZG)4. For DTG curves, it can be seen that there are three degradation stages at about 66 °C, 361 °C and 409 °C for p(AAPBA), and 195 °C, 349 °C and 418 °C for p(AAPBA-b-OVZG)4. For p(AAPBA-b-OVZG)4, the first peak at 195 °C is assigned to loss of free water and water linked through hydrogen bonds. The second peak, which has a maximum around 361 °C for p(AAPBA) and 349 °C for p(AAPBA-b-OVZG)4, corresponds to the thermal decomposition of the pendent residues. The last degradation stage involves thermal degradation of the backbone and shows a peak at 409 °C for p(AAPBA) and 418 °C for p(AAPBA-b-OVZG)4. These results are consistent with previous reports [29] and show that the copolymer structure plays an important role in their thermal decomposition and stability.

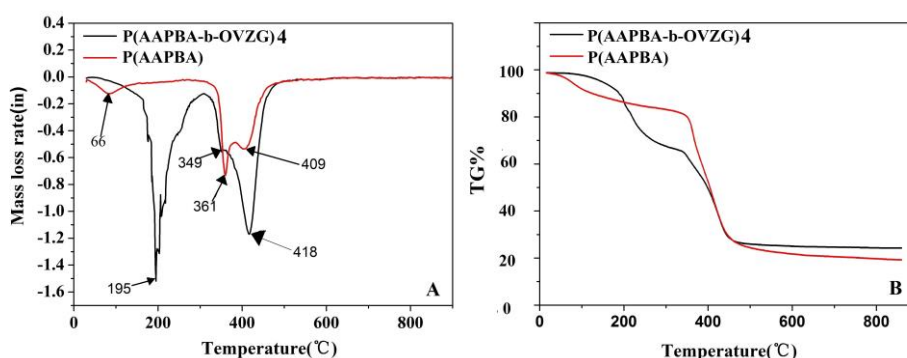


Fig.3. Thermal analysis of the copolymers: (A) DTG and (B) TG

The molecular weights of the polymers determined by GPC are summarized in Table 2. It was found that a higher p(AAPBA) ratio in the p(AAPBA-b-OVZG) co-polymer leads to an increase of M_w , M_n and PDI. This was also found in our previous work [21], where the new compound p(N-vinylcaprolactam-co-3-acrylamidophenylboronic acid) had higher M_w , M_n and PDI as the proportion of AAPBA increased.

Table2. The molecular weights (M_w and M_n) and molecular weight distributions of the copolymers

Sample	OVZG/(pAAPBA)	M_w	M_n	PDI
p(AAPBA-b-OVZG)1	100/10	66754	54202	1.23
p(AAPBA-b-OVZG)2	100/20	69568	56572	1.23
p(AAPBA-b-OVZG)3	100/50	71348	58792	1.21
p(AAPBA-b-OVZG)4	100/100	78522	64892	1.21
p(AAPBA-b-OVZG)5	100/200	84892	70454	1.20

3.2 Nanoparticle characterization

Photographs of suspensions of the different p(AAPBA-b-OVZG) NPs (1mg/mL) and the TEM images of all the NPs can be seen in the Fig.S1 and the degradation characteristics of the polymers in vitro at 37 °C can be seen in Fig S3. In addition, Fig. 4 indicates that the size of the blank NPs (no insulin) change very little over 6 weeks, indicating that p(AAPBA-b-OVZG) NPs are stable in aqueous solution. Fig S2 illustrates the change in hydrodynamic diameters at different pH values indicating the optimal ratio of OVZG to p(AAPBA) NPs.

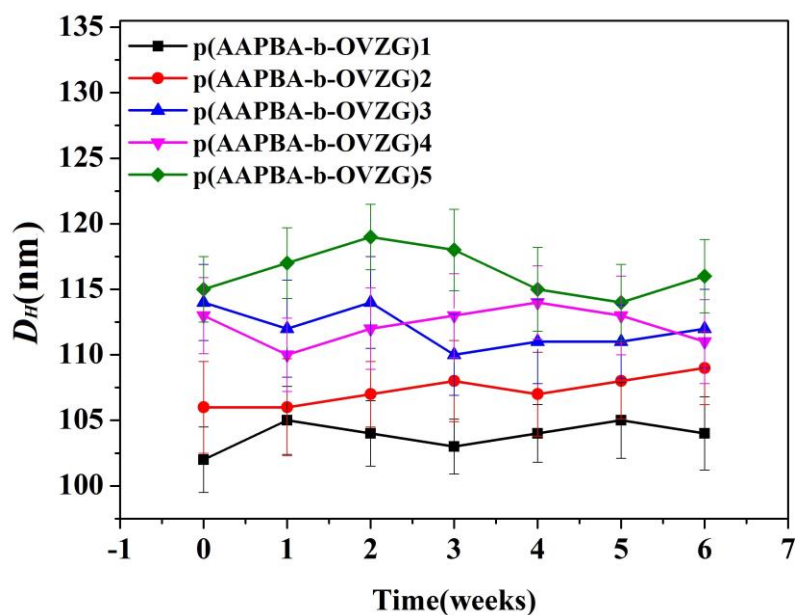


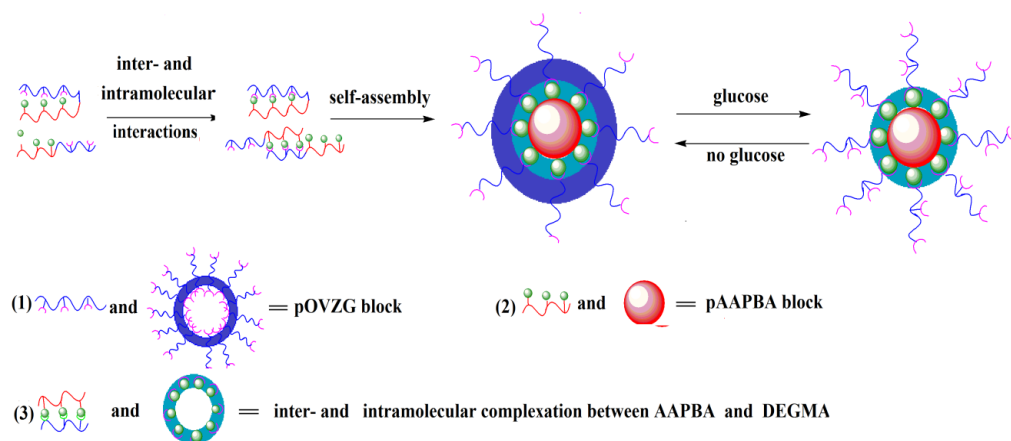
Fig.4. The stability of blank p(AAPBA-b-OVZG) NPs in pH 7.4 PBS.

Moreover, it was found that with the increase of the p(AAPBA) ratio in the p(AAPBA-b-OVZG) co-polymer, the Zeta potential (determined with a submicron particle size analyzer; ZetaPALS/90plus, Brookhaven Instruments Corporation, Holtsville, NY, USA) was decreased from -21.4 to -36.3 and this trend has been observed previously [29-30]. Overall, the nanoparticles become more and more stable with a higher proportion of p(AAPBA). (Table 3).

Tab.3. The zeta potentials of the copolymer NPs.

Samples	OVZG/(pAAPBA)	Zeta potential (mV)
p(AAPBA-b-OVZG)1	100/10	-21.4±2.3
p(AAPBA-b-OVZG)2	100/20	-26.9±1.8
p(AAPBA-b-OVZG)3	100/50	-33.6±1.7
p(AAPBA-b-OVZG)4	100/100	-34.2±0.9
p(AAPBA-b-OVZG)5	100/200	-36.3±1.2

The mechanism proposed for the glucose-responsive nature of the materials is summarized in Scheme 3.



Scheme 3. Schematic representation of nanoparticles

Fig. 5 shows the hydrodynamic diameters of nanoparticles in the glucose medium (on the left) and the values of I/I_0 versus time in pH 7.4 PBS (on the right). They were measured by DLS where I represent the light scattering intensity and I_0 is the control value of the nanoparticles in the absence of glucose. The values of I/I_0 agree with previously reported data on the nanoparticle swelling degree in different glucose media [31]. From Fig.5 A1 to Fig.5 A5 it can be seen that in the absence of glucose the hydrodynamic diameters do not change much over 60 min but as the glucose concentration is increased there is a trend toward bigger diameters as the amount of pAAPBA present is increased. Fig.5 B1 to Fig.5 B5 shows, that there is a decreasing trend in the I/I_0 ratio as the glucose concentration was changed from 0 to 3 mg/mL. The reduction in the I/I_0 values was greater in the 3 mg/mL glucose medium than in 0 mg/mL for each type of nanoparticle due to more dissociation of nanoparticles at higher glucose concentration [32]. Furthermore, the

pattern of the hydrodynamic diameter enhancement showed the glucose sensitivity since the glucose combined with the boronic acid moieties forming a boronate complex [33], which was dynamically-covalent, and allowed the linkage to reconfigure in presence of other polyols such as glucose. Interestingly, p(AAPBA-b-OVZG)5 showed hardly any change in size compared with p(AAPBA-b-OVZG)4 possibly due to the fact that the AAPBA in p(AAPBA-b-DEGMA)5 cannot be ionized any further.

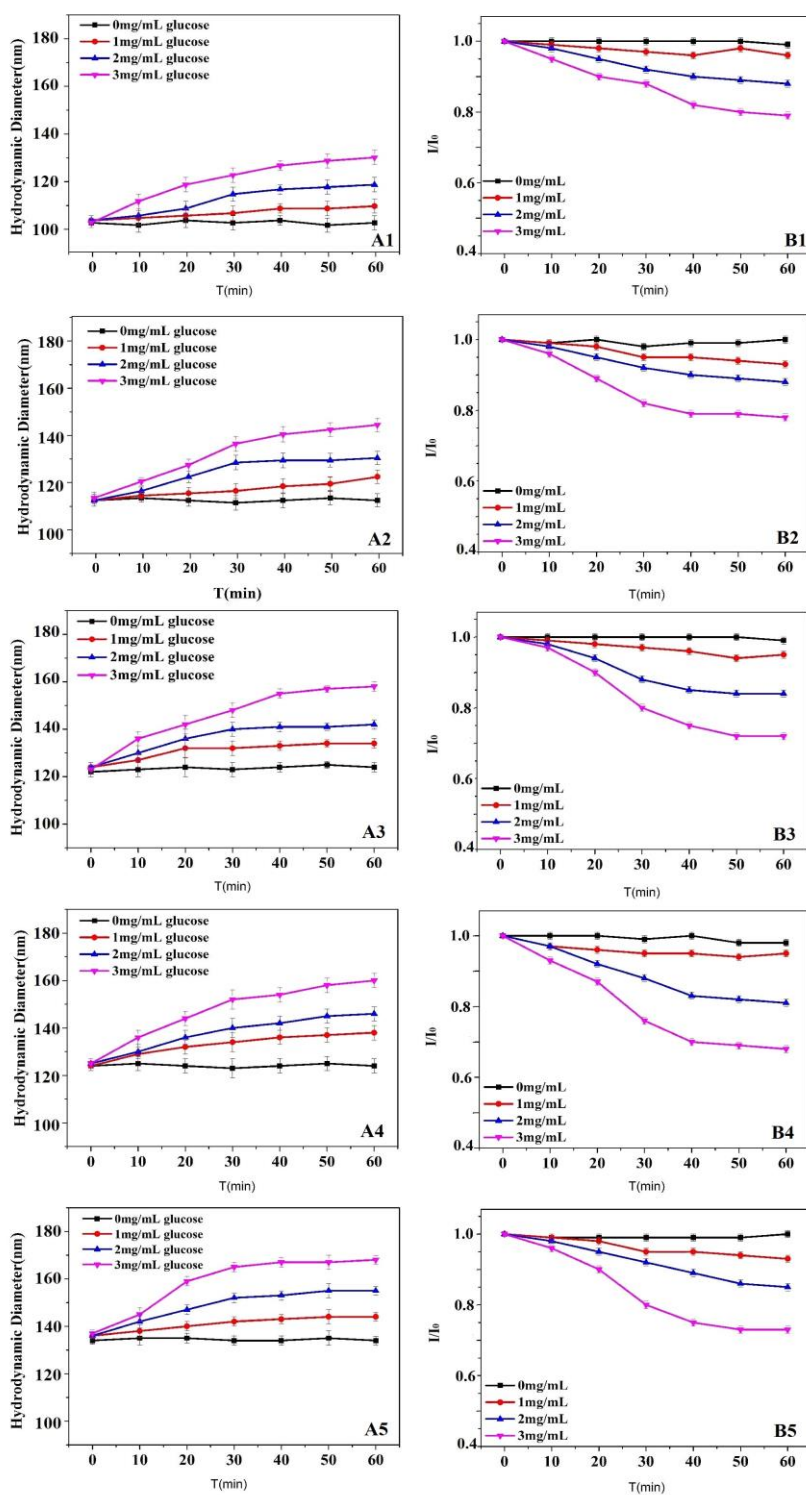


Fig.5. Changes in the size of the p(AAPBA-b-OVZG) nanoparticles as a function of immersion time in pH 7.4 PBS solutions of glucose. (1) p(AAPBA-b-OVZG)1; (2) p(AAPBA-b-OVZG)2; (3) p(AAPBA-b-OVZG)3; (4) p(AAPBA-b-OVZG)4; (5) p(AAPBA-b-OVZG)5. The graphs on the left (marked A) show the hydrodynamic

diameters, while those on the right (marked B) show I/I_0

Fig. 6 illustrates that the glycopolymers show reversible glucose sensitivity. All of the p(AAPBA-b-OVZG) samples swelled after the first treatment with 3 mg/mL glucose for 4h, and then they contracted virtually to their original size when placed in water containing no glucose. When treated with glucose (3 mg/mL) for the second time, the NPs swelled again and returned to a size, which was close to the first swelling.

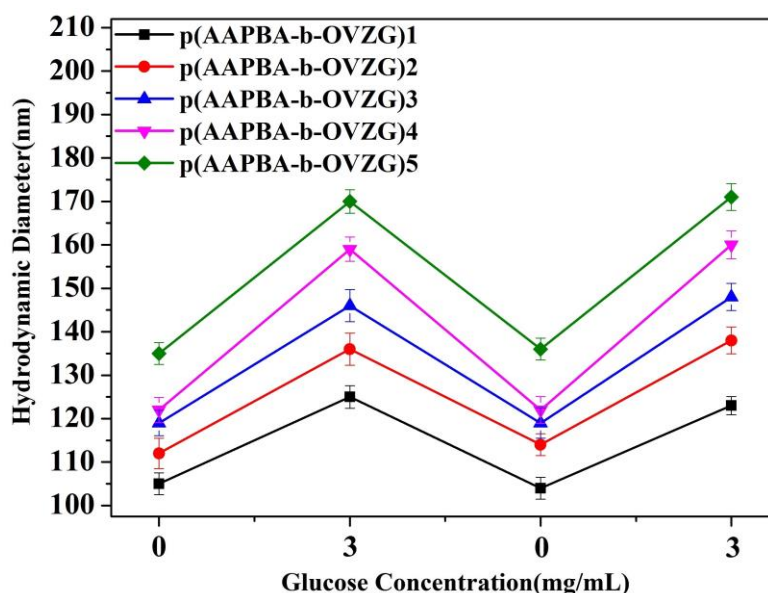


Fig.6. Reversible glucose sensitivity of p(AAPBA-b-OVZG) NPs.

3.4 Insulin loading and release

The self-assembly process can be influenced by hydrophobic–hydrophilic interactions, electrostatic interactions, hydrogen bonding and other intermolecular interactions [34]. Insulin, a protein containing numerous amino acids, has hydrophilic and hydrophobic residues and can form stable complexes due to the above interactions [35]. Thus, when added to p(AAPBA-b-OVZG) suspension of nanoparticles and coupled with the amphiphilic glycopolymer, insulin can be loaded

onto the glycopolymer NPs via hydrogen bonding, van der Waals forces and hydrophilic–hydrophobic interactions [36]. The results in Table 4 show that insulin was easily attached to the p(AAPBA-b-OVZG) NPs and the loading capacity of insulin was about 10% for all NPs and the encapsulation efficiency of insulin increased from 53.2% to 63.8% as the ratio of pAAPBA was raised.

Tab.4. Insulin loading capacity and encapsulation efficiency of p(AAPBA-b-OVZG) NPs

Samples	LC%	EF%
p(AAPBA-b-OVZG)1	9.81+3.43	58.49+2.41
p(AAPBA-b-OVZG)2	10.23+2.87	60.22+3.26
p(AAPBA-b-OVZG)3	11.36+3.01	57.52+1.92
p(AAPBA-b-OVZG)4	11.42+2.85	64.31+3.14
p(AAPBA-b-OVZG)5	11.22+3.23	55.33+2.76

All of the p(AAPBA-b-OVZG) NPs were able to detect the amount of insulin release at different glucose concentrations. It can be seen from Fig.7A that the cumulative release of insulin from the p(AAPBA-b-OVZG)4 NPs increased at higher glucose concentrations and Fig.7B shows that the best results are obtained using p(AAPBA-b-OVZG)4 NPs in 3mg/mL glucose solution. It can also be seen that the release of insulin continues for around 120 h and compared with the reports of Yao et al. and Arjyabaran Sinha et al. [36-37] this is a considerable enhancement. Yao et al. fabricated [37] the amphiphilic block copolymer poly(ethylene glycol)-block-poly((2-phenylboronic ester-1,3 -dioxane-5-ethyl) methylacrylate) (MPEG5000-b-PBDEMA) via atom transfer radical polymerization (ATRP) using MPEG5000-Br

as a macroinitiator and found the time of cumulative release of insulin was reached at 60 h in 3 mg/mL of glucose solution. Arjyabaran Sinha et al. [38] designed a phenylboronic acid functionalized MMS (MMS-PBA) but found the time of cumulative release was only 8 h in 3mg/mL of glucose solution.

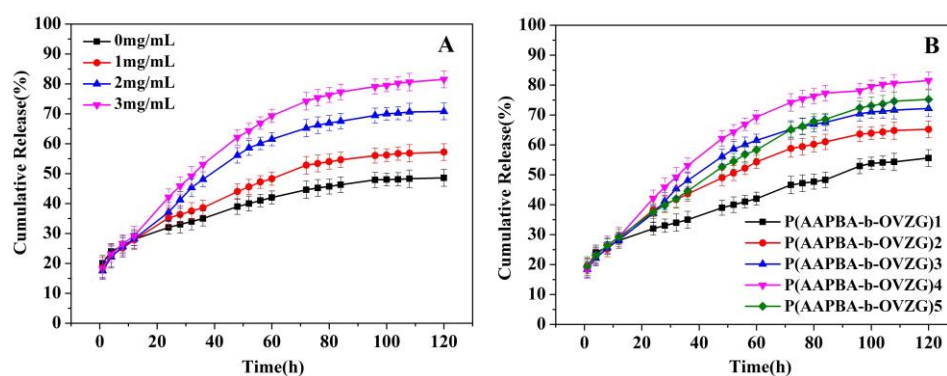


Fig.7. In vitro cumulative release of insulin in pH 7.4 PBS from: (A) p(AAPBA-b-OVZG)4 in different concentrations of glucose in solution, and (B) p(AAPBA-b-OVZG)1, p(AAPBA-b-OVZG)2, p(AAPBA-b-OVZG)3, p(AAPBA-b-OVZG) 4 and p(AAPBA-b -OVZG)5 in 3 mg/mL glucose solution.

In order to elucidate the insulin release mechanism, the results were analyzed in the light of the Ritger-Peppas equation. R^2 values higher than 0.9 were obtained and the values of n were in the range 0.29–0.54 (Table 5) indicating that insulin release was mainly due to non-Fickian diffusion.

Tab.5. Drug Release Kinetic Data for the Copolymer Nanoparticles Obtained from Fitting Drug Release Data to the Ritger-Peppas Equation (where n is the diffusion exponent; k is the kinetic constant; R² is correlation coefficient.)

samples	glucose concentration (mg/mL)	Ritger-Peppas model			transport mechanism
		n	k	R ²	
p(AAPBA-b-OVZG)1	3	0.2943	23.816	0.9789	non-Fickian diffusion
p(AAPBA-b-OVZG)2	3	0.3901	26.606	0.9267	non-Fickian diffusion
p(AAPBA-b-OVZG)3	3	0.4647	26.971	0.9059	non-Fickian diffusion
p(AAPBA-b-OVZG)4	3	0.5447	28.513	0.9035	non-Fickian diffusion
p(AAPBA-b-OVZG)5	3	0.4906	25.316	0.9591	non-Fickian diffusion

CD spectroscopy was employed to evaluate the insulin conformational changes. The far-UV-CD band at 208 nm primarily arises from an α -helix structure, while the β -structure caused the band at 223 nm. The changes in the ratio of $[F]_{208}/[F]_{223}$ can be used to evaluate any alterations in conformation. The ratio of $[F]_{208}/[F]_{223}$ was found to be 1.28 and 1.21 for standard insulin and released insulin, indicating that there was no significant conformational change observed for the insulin released from the NPs at pH 7.4 in contrast to standard insulin (Fig. 8). Furthermore, the spectral characteristics show that the release process did not distort the tertiary structure of insulin.

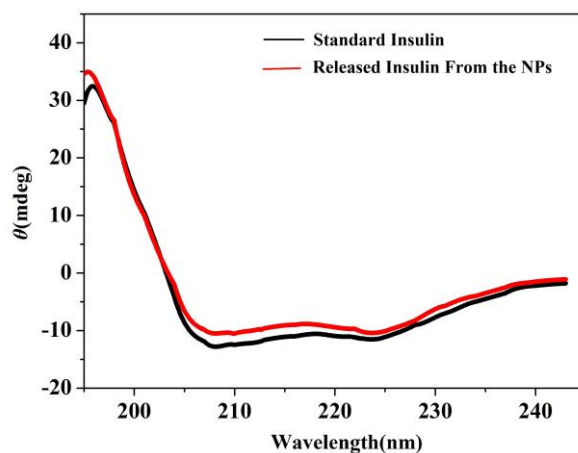


Fig.8. CD spectra of the insulin released from the nanoparticles and standard insulin in PBS at pH 7.4, 25 °C.

3.5 Cytotoxicity testing

Fig.9 shows the cytotoxicity of blank nanoparticles and p(AAPBA-b-OVZG) NPs as determined by the MTT method on NIH3T3 cell lines. The NIH3T3 cells were exposed to suspensions of the NPs at concentrations varying from 20 to 120 $\mu\text{g/mL}$ and the cells without pretreatment were set as a negative control group. The relative cell viability of the samples was higher than 80% after incubating for 24 h, indicating that the presence of the glycopolymer had no negative influence on cell viability although the cell viability was the highest when the AAPBA content in the glycopolymer was the lowest. Overall, those results suggested that the OVZG moieties in the polymers reduced the cytotoxicity and the presence of phenylboronic acid enhanced the glucose-sensitivity of the polymers. As a result, those nanoparticles have little cytotoxicity and favorable biocompatibility, indicating a potential application for insulin delivery *in vivo*.

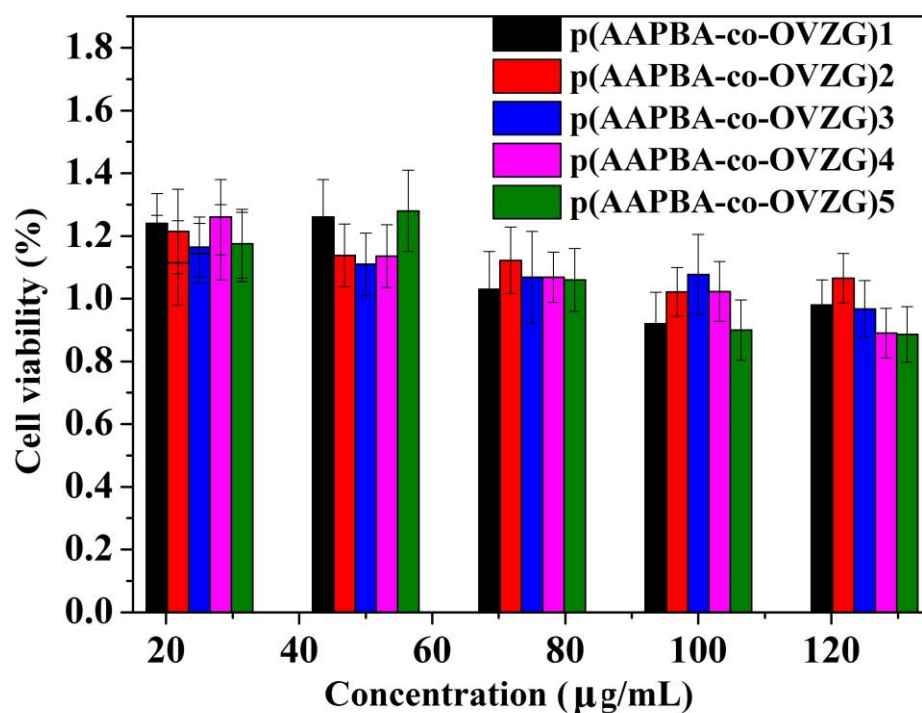


Fig.9. Cell viability using the MTT assay at 37 °C after the incubation for 24 h as a function of the concentration of

p(NVCL-co-AAPBA) NPs. Each value represents the mean \pm SD (n=5)

3.6 Animal toxicity

Before the nanoparticles are injected to animals or patients, cell and animal toxicity needs to be determined. Many studies have shown that PBA based co-polymers or nanogels have good cytocompatibility [39; 40] and our research is consistent with these reports. For animal toxicity, previous research has found that the PBA has a certain level of toxicity [41; 42], but if the PBA is incorporated into a copolymer, then the situation may change considerably. Fig. 10 shows the testing results obtained from intraperitoneally injecting 100, 200 and 400 mg/kg/d of NPs according to the weight of the mice. Silky hair was found to be present in all of the mice, there appeared to be good mental state and regular eating and drinking habits during 7 days observation. A total of 7 days later, all the mice were sacrificed; their livers, kidneys, hearts, spleens and lungs

were harvested for HE staining. It can be seen in Fig. 10 that the tissues were not obviously damaged, indicating that the prepared materials had no toxicity *in vivo* in short term.

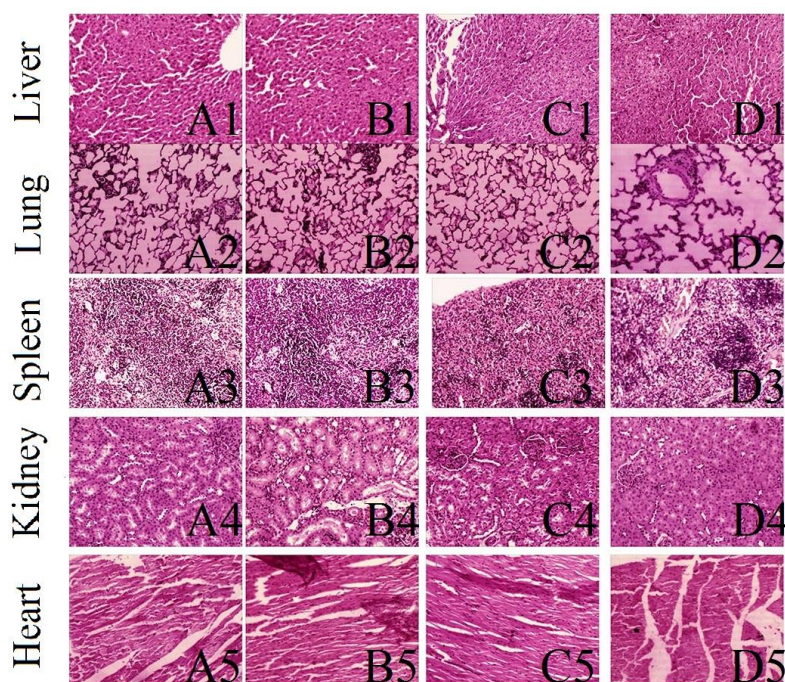


Fig.10. Representative images of HE staining results from (A) the control group; (B) the observation group (100mg); (C) the observation group (200mg); (D) the observation group (400mg) on (1) liver; (2) kidney; (3) lung; (4) spleen; (5) heart

Also, in separate a chronic toxicity trial mice received intraperitoneal injections of 10, 20 and 40 mg/kg/d of NPs respectively. These results demonstrate that the materials are safe and have no adverse influence on the blood biochemical values, indicating that the materials have no toxicity over at least 60 days *in vivo* (Table 6).

Tab.6. Effect of administration by injection of the NPs on the biochemical parameters of rats after 60 d (n=5, mean±SD)

parameter	Control Group	Observation group(mg/kg)		
		10	20	40
RBC($\times 10^6$ /uL)	2.85±0.23	2.92±0.19	2.89±0.20	2.94±0.23
WBC($\times 10^3$ /uL)	9.42±0.39	9.57±0.48	9.64±0.51	9.72±0.28
Haemoglobin(g/dl)	14.44±1.19	14.62±1.70	14.58±1.18	14.52±1.19
Haematocrit(vol.%)	36.57±1.22	36.76±1.29	36.57±1.39	36.68±1.38
Platelet($\times 10^3$ /uL))	88.77±2.72	91.14±2.08	92.23±2.41	92.42±2.47
Serum protein (g/l)	55.82±3.41	55.61±3.49	56.86±2.81	56.28±2.86
Serum creatinine (mg/dl)	3.52±0.19	3.64±0.18	3.69±0.25	3.71±0.27
Serum glutathione (mg/dl)	0.61±0.05	0.67±0.11	0.59±0.12	0.57±0.21
Total cholesterol (mg/dl)	71.23±4.46	70.43±4.78	68.98±4.83	70.11±5.12
Glucose (mg/dl)	262.43±9.05	259.26±8.34	258.17±9.12	251.21±8.75
Uric acid (mg/dl)	5.19±0.69	5.24±0.58	5.29±0.59	5.31±0.61
AST(U/l)	39.18±3.31	40.23±3.51	41.42±3.49	39.87±3.32
ALT(U/l)	95.87±4.71	96.17±4.53	96.23±4.28	97.16±4.47

3.7 In vivo hypoglycemic studies

To date, much work has been carried out on rats or mice via oral administration of insulin loaded NPs. Guo et al. [43] prepared the amphiphilic glycopolymer poly(D-gluconamidoethyl

methacrylate-random-3-acrylamidophenyl boronic acid) (p(GAMA-r-AAPBA)) and found there was a significant decrease in blood glucose levels after oral administration. These results are consistent with those of Zhang et al. [44] and Sun et al. [45], who demonstrated that appropriately loaded oral nanoparticles can effectively lower blood sugar. Other work by Wu et al. [40] reported that the nanogels of poly(N-isopropylacrylamide), dextran and poly(3-acrylamidophenylboronic acid) (p(NIPAM-Dex-PBA)) could decrease blood glucose levels in diabetic rats and 51% of the baseline level was maintained for almost 2 hours. In the present study, the plasma of diabetes mice was periodically collected from the tail veins at 0, 1, 2, 3, 4, 5, 6, 12, 24, 36, 48, 60, 72, 84, 96, 108 and 120 h in order to quantify glucose levels. The results (Fig. 11A) reveal that the insulin-loaded NPs and insulin injection-treated mice had similar glucose levels from 0 h to 96 h, while the former showed a slight increase in blood glucose levels after 100 h. This suggests that insulin-loaded NPs have a consistent hypoglycemic effect on the mice at least for 96 hours. Additionally, Fig 11B indicates that the plasma glucose levels were rapidly downregulated in insulin injection-treated groups and insulin-loaded NPs groups and this is consistent with the studies mentioned above [21,40]. This demonstrates that AAPBA, as a part of the p(AAPBA-b-OVZG) polymer, shows excellent sensitivity to glucose and this effect is almost equivalent to that of insulin injection-treated groups over 96 h.

After injecting the mice with the NPs, the released insulin can be used to determine the relative bioavailability [46, 47]. Lei et al. [48] manufactured a composite hydrogel system containing glucose-responsive nanocarriers for oral delivery of insulin and found the glucose-responsive nanocarriers can significantly prolong the time of insulin in the serum. In addition, Depeng et al. [49] fabricated a CaCO₃-based composite nanocarrier and got the same results and similar studies

have also been conducted [50-52]. Fig.11C and Fig.11D shows that the insulin levels were about 19~25 mIU/L in the control group and were about 10~15 mIU/L in the diabetic group indicating that both insulin injection treatment and the insulin-loaded NPs groups show a sharp increase in the plasma insulin concentration. Meanwhile, for the insulin injection treatment group, the highest value is seen after a short time (~2 h) and then decreases rapidly to a lower level within 4 h. In contrast, for the NPs group the plasma insulin concentration is increased to the highest value at 3h and then declined slowly to a lower level after 80 h. These results demonstrate that the insulin-loaded NPs have an obvious advantage compared with insulin injection.

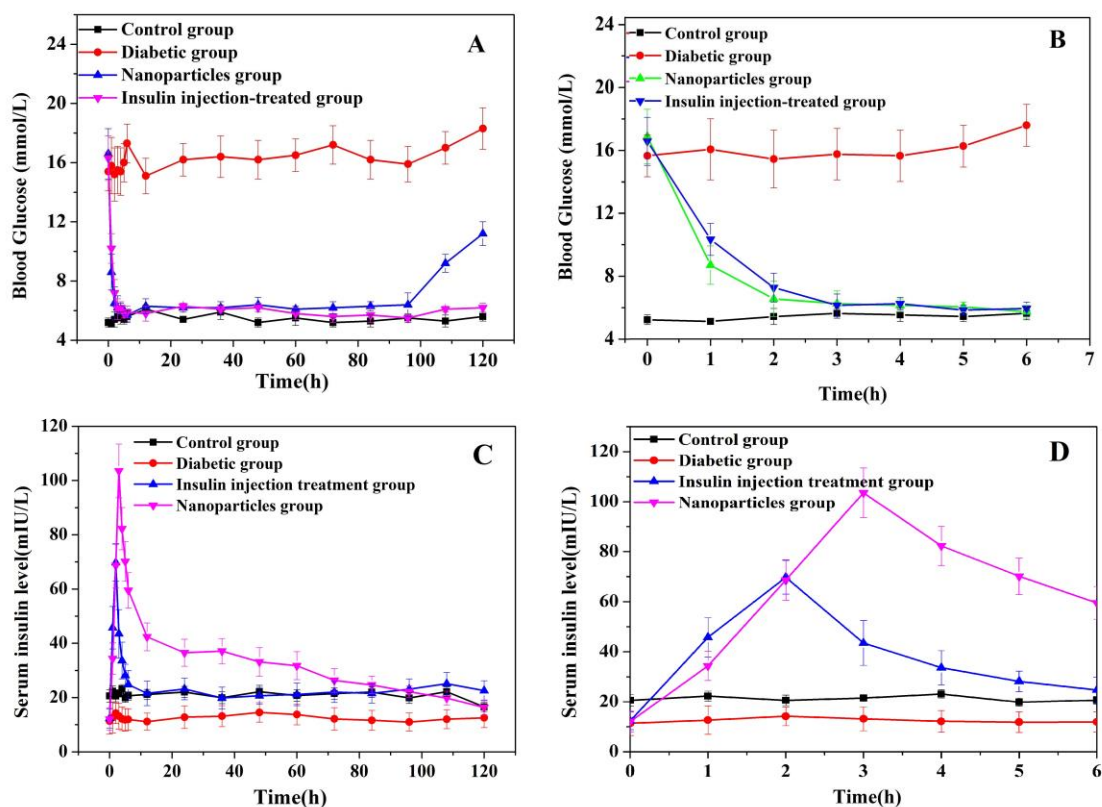


Fig.11. Blood glucose and serum insulin concentration after injection: A over 120 h and B over 6 h. (Fig.13 does not show the hypoglycemic effect within first six hours, so this is presented over 6 h in Fig.13B; Fig.13C is presented over 6 h in Fig.13D;).

4. Conclusions

A novel amphiphilic block glycopolymer, p(AAPBA-b-OVZG) based on phenylboronic acid and 6-O-vinylazeloxy-D-galactose was synthesized. The Mw, Mn and PDI increased as the ratio of p(AAPBA) present was elevated in p(AAPBA-b-OVZG). The polymers have an ability to easily self-assemble into spherical NPs (50-250nm) which exhibited excellent glucose-sensitive behavior at physiological pH *in vivo*. In the presence of increasing glucose levels in solution the size of NPs became larger. Insulin was easily encapsulated into the NPs, with a high loading capacity of 10% and it was found that the release of insulin is in response to an increased glucose concentration. Moreover it was found that the glycopolymers have an ideal biocompatibility both *in vitro* and *in vivo*, indicating a potential application in the biomedical field as the persistent hypoglycemic effect of p(AAPBA-b-OVZG) NPs were effective over 96h. Taken together, this study suggests that promising glycopolymers based on p(AAPBA-b-OVZG) may be applied as an insulin delivery system in the future.

6. Acknowledgements

This investigation was supported by the grant 16410723700 from the Science and Technology Commission of Shanghai Municipality, the Biomedical Textile Materials “111 Project” of the Ministry of Education of China (No. B07024), and the UK-China Joint Laboratory for Therapeutic Textiles (based at Donghua University)

References

- [1] Oyer, D. S., Shepherd, M. D., Coulter, F. C., Bhargava, A., Deluzio, A. J., Chu, P. L.. Efficacy and tolerability of self-titrated biphasic insulin aspart 70/30 in patients aged >65 years with type 2 diabetes: an exploratory post hoc sub-analysis of the INITIATEplus trial. *Clinical Therapeutics*, 33(2011), 874–883.
- [2] Zia, A., Bhatti, A., Jalil, F., Wang, X., John, P., Kiani, A. K.. Prevalence of type 2 diabetes–associated complications in pakistan. *International Journal of Diabetes in Developing Countries*, 36(2016), 1-10.
- [3] Krug, E. G.. Trends in diabetes: sounding the alarm. *Lancet*, 387(2016), 1485-1486.
- [4] Zhou, B., Lu, Y., Hajifathalian, K., Bentham, J., Cesare, M. D., Danaei, G.. Worldwide trends in diabetes since 1980: a pooled analysis of 751 population-based studies with 4.4 million participants. *Lancet*, 387(2016), 1513-1530.
- [5] Backes, J. M., Kostoff, M. D., Gibson, C. A., & Ruisinger, J. F.. Statin-associated diabetes mellitus: review and clinical guide. *Southern Medical Journal*, 109(2016), 167-173.
- [6] Zaletel, J., Piletic, M., Lindström, J., Icks, A., Rothe, U., Sørensen, M., et al.. National diabetes plans: can they support changes in health care systems to strengthen diabetes prevention and care? *Annali Dellistituto Superiore Di Sanita*, 51(2015), 206-208.
- [7] Shavandi, N., Shahrjerdi, S., Hoseini, R. S., & Ghorbani, A.. The effect of strengthening exercises on metabolic factors, quality of life and mental health in women with type 2 diabetes. *Iranian Journal of Endocrinology & Metabolism*, 12(2010), 300-310.
- [8] Lee, S. S., & Kang, S.. Effects of regular exercise on obesity and type 2 diabetes mellitus in korean children: improvements glycemic control and serum adipokines level. *Journal of*

- Physical Therapy Science*, 27(2015), 1903-1907.
- [9] Wu, J., Williams, G. R., Branford-White, C., Li, H., Yan, L., & Zhu, L. M.. Liraglutide-loaded poly(lactic-co-glycolic acid) microspheres: preparation and in vivo, evaluation. *European Journal of Pharmaceutical Sciences*, 92(2016), 28-38.
- [10] Silverstone, F. A., Brandfonbrener, M., Shock, N. W., Yiencst, M. J.. Age differences in intravenous glucose tolerance tests and response to insulin. *Journal of Clinical Investigation*, 36(1957), 504-514.
- [11] Alexander, J. S., Ganta, V. C., Jordan, P. A., Witte, M. H.. Gastrointestinal lymphatics in health and disease. *Pathophysiology*, 17(2010), 315-335.
- [12] Zhao, W., Li, J., Jin, K., Liu, W., Qiu, X., & Li, C. Fabrication of functional PLGA-based electrospun scaffolds and their applications in biomedical engineering[J]. *Materials Science & Engineering C*, 2016, 59(2016):1181-1194.
- [13] Li, L., Jiang, G., Jiang, T., Huang, Q., Chen, H., Liu, Y. Preparation of dual-responsive nanogels for controlled release of insulin. *Journal of Polymer Materials*, 32 (2015), 77-84.
- [14] Shahzad, S., Shahzadi, L., Mahmood, N., Siddiqi, S. A., Rauf, A., Manzoor, F.. A new synthetic methodology for the preparation of biocompatible and organo-soluble barbituric- and thiobarbituric acid based chitosan derivatives for biomedical applications. *Materials Science & Engineering C*, 66(2016), 156-163.
- [15] Chai, Z., Ma, L., Wang, Y., Ren, X.. Phenylboronic acid as a glucose-responsive trigger to tune the insulin release of glycopolymer nanoparticles. *Journal of Biomaterials Science Polymer Edition*, 57(2016), 1-26.
- [16] Lei, L., Jiang, G., Yu, W., Liu, D., Hua, C., Liu, Y.. A composite hydrogel system containing

- glucose-responsive nanocarriers for oral delivery of insulin. *Materials Science & Engineering C*, 69(2016), 37-45.
- [17] Seno, M., Yoshida, K., Sato, K., Anzai, J.. pH- and sugar-sensitive multilayer films composed of phenylboronic acid (pba)-modified poly(allylamine hydrochloride) (pba-pah) and poly(vinyl alcohol) (pva): a significant effect of pba content on the film stability. *Materials Science & Engineering C*, 62(2016), 474-479.
- [18] Sun, L., Huang, W. M., Ding, Z., Zhao, Y., Wang, C. C., Purnawali, H.. Stimulus-responsive shape memory materials: a review. *Materials & Design*, 33(2012), 577-640.
- [19] Wang, D., Liu, T., Yin, J., Liu, S.. Stimuli-responsive fluorescent poly(N-isopropylacrylamide) microgels labeled with phenylboronic acid moieties as multifunctional ratiometric probes for glucose and temperatures. *Macromolecules*, 44(2011), 2282-2290.
- [20] Sun, L., Zhang, X., Zheng, C., Wu, Z., Xia, X., Li, C.. Glucose- and temperature-responsive core-shell microgels for controlled insulin release. *RSC Advances*, 2(2012), 9904-9913.
- [21] Wu, J. Z., Bremner, D. H., Li, H. Y., Sun, X. Z., & Zhu, L. M.. Synthesis and evaluation of temperature- and glucose-sensitive nanoparticles based on phenylboronic acid and N-vinylcaprolactam for insulin delivery. *Materials Science & Engineering C*, 69(2016), 1026-1035.
- [22] Ladmiral, V., Melia, E., Haddleton, D. M.. Synthetic glycopolymers: an overview. *European Polymer Journal*, 40(2004), 431-449.
- [23] Guo, Q., Zhang, T., An, J., Wu, Z., Zhao, Y., ai, X., et al.. Block versus random amphiphilic glycopolymer nanoparticles as glucose-responsive vehicles. *Biomacromolecules*, 16(2015), 3345-3356.

- [24] Sun, K., Bligh, S. W. A., Nie, H., Quan, J., Zhu, L. Lectin recognizing thermoresponsive double hydrophilic glycopolymer micelles by raft polymerization. *RSC Advances*, 4(2014), 34912-34921.
- [25] Xing, S., Guan, Y., & Zhang, Y.. Kinetics of glucose-induced swelling of p(nipam-aapba) microgels. *Macromolecules*, 44(2011), 4479-4486.
- [26] Sun, K., Xu, M., Zhou, K., Nie, H., Quan, J., Zhu, L. Thermoresponsive diblock glycopolymer by raft polymerization for lectin recognition. *Materials Science & Engineering C*, 68(2016), 172-176.
- [27] Guo Q, Wu Z, Zhang X. Phenylboronate-diol crosslinked glycopolymeric nanocarriers for insulin delivery at physiological pH. *Soft Matter*, 10(2014):911-920.
- [28] Jin, X., Zhang, X., Wu, Z., Teng, D., Zhang, X., Wang, Y., et al. Amphiphilic random glycopolymer based on phenylboronic acid: synthesis, characterization, and potential as glucose-sensitive matrix. *Biomacromolecules*, 10(2009), 1337-1345.
- [29] Li, C., Liu, Z., Yan, X., Lu, W., Liu, Y. Mucin-controlled drug release from mucoadhesive phenylboronic acid-rich nanoparticles. *International Journal of Pharmaceutics*, 479(2014), 261-264.
- [30] Hasegawa, U., Inubushi, R., Uyama, H., Uematsu, T., Kuwabata, S., van der Vlies, A. J. Mannose-displaying fluorescent framboidal nanoparticles containing phenylboronic acid groups as a potential drug carrier for macrophage targeting. *Colloids and Surfaces B: Biointerfaces*, 136 (2015), 1174-1181.
- [31] Ma, R., Yang, H., Li, Z., Liu, G., Sun, X., Liu, X.. Phenylboronic acid-based complex micelles with enhanced glucose-responsiveness at physiological pH by complexation with

- glycopolymer. *Biomacromolecules*, 13(2012), 3409-3417.
- [32] Wang, B., Ma, R., Liu, G., Li, Y., Liu, X., An, Y.. Glucose-responsive micelles from self-assembly of poly(ethylene glycol)-b-poly(acrylic acid-co-acrylamidophenylboronic acid) and the controlled release of insulin. *Langmuir*, 25(2009), 12522-12528.
- [33] Wang, Y., Chai, Z., Wang, N., Sun, Y., Yan, Y., Gao, L.. Multiple sensitivity study of boronic acid-functionalized nanoparticles based on the complexation of poly (3-methacrylamidophenylboronic acid) and dextran. *Journal of Macromolecular Science Part A*, 52(2015), 267-272.
- [34] Moreau, J. J. E., Luc, V., Michel, W. C. M., Catherine, B., Philippe, D., Jean - Louis, B... Lamellar bridged silsesquioxanes: self-assembly through a combination of hydrogen bonding and hydrophobic-interactions. *Chemistry*, 11(2005), 1527-1537.
- [35] Shuyi, H., Sasa, C., Yuming, W., Jiqian, W., Daohong, X., Hai, X.. Self-assembly of short peptide amphiphiles: the cooperative effect of hydrophobic interaction and hydrogen bonding. *Chemistry - A European Journal*, 17(2011), 13095-13102.
- [36] Lian, Y., Zhao, K.. Study of micelles and microemulsions formed in a hydrophobic ionic liquid by a dielectric spectroscopy method. 1. interaction and percolation. *Soft Matter*, 7(2011), 8828-8837.
- [37] Yao, Y., Zhao, L., Yang, J., Yang, J.. Glucose-responsive vehicles containing phenylborate ester for controlled insulin release at neutral pH. *Biomacromolecules*, 13(2012), 1837-1844.
- [38] Sinha, A., Chakraborty, A., Jana, N. R.. Dextran-gated, multifunctional mesoporous nanoparticle for glucose-responsive and targeted drug delivery. *ACS Applied Materials & Interfaces*, 6 (2014), 22183-22191.

- [39] Yuan, Y., Shen, H., Zhang, G., Jing, Y., Xu, J.. Synthesis of poly(N-isopropylacrylamide)-co-poly(phenylboronate ester) acrylate and study on their glucose-responsive behavior. *Journal of Colloid & Interface Science*, 431(2014), 216-222.
- [40] Wu, Z., Zhang, X., Guo, H., Li, C., Yu, D.. An injectable and glucose-sensitive nanogel for controlled insulin release. *Journal of Materials Chemistry*, 22(2012), 22788-22796.
- [41] Lee, I. P., Sherins, R. J., Dixon, R. L.. Evidence for induction of germinal aplasia in male rats by environmental exposure to boron. *Toxicology and Applied Pharmacology*, 45(1978), 577-590.
- [42] Chapin R E, Ku W W..The reproductive toxicity of boric acid. *Environmental Health Perspectives*, 102 (1994):87-91.
- [43] Guo, H., Li, H., Gao, J., Zhao, G., Ling, L., Wang, B., Li, C.. Phenylboronic acid-based amphiphilic glycopolymeric nanocarriers for in vivo insulin delivery. *Polymer Chemistry*, 7(2016), 3189-3199.
- [44] Zhang, Y., Liu, K., Guan, Y., Zhang, Y.. Assembling of gold nanorods on p(nipam-aapba) microgels: a large shift in the plasmon band and colorimetric glucose sensing. *RSC Advances*, 2(2012), 4768-4776.
- [45] Sun, L., Zhang, X., Wu, Z., Zheng, C., Li, C.. Oral glucose- and pH-sensitive nanocarriers for simulating insulin release in vivo. *Polym Chem*, 5(2014), 1999-2009.
- [46] Li, L., Jiang, G., Yu, W., Liu, D., Chen, H., Liu, Y. Preparation of chitosan-based multifunctional nanocarriers overcoming multiple barriers for oral delivery of insulin. *Materials Science & Engineering C*, 70 (2017), 278-286.
- [47] Yu, W., Jiang, G., Liu, D., Lei, L., Hua, C., Liu, Y. Fabrication of biodegradable composite

microneedles based on calcium sulfate and gelatin for transdermal delivery of insulin.

Materials Science & Engineering C, 71 (2017), 725–734.

[48] Lei, L., Jiang, G., Yu, W., Liu, D., Hua, C., Liu, Y. A composite hydrogel system containing glucose-responsive nanocarriers for oral delivery of insulin. *Materials Science & Engineering C*, 69(2016), 37-45.

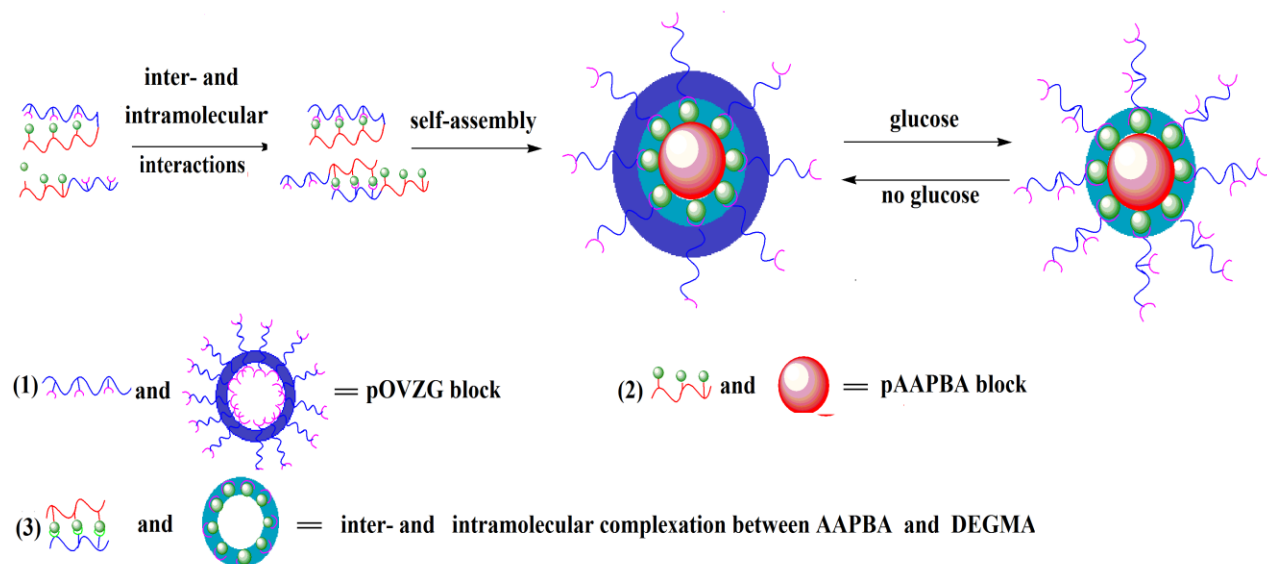
[49] Liu, D., Jiang, G., Yu, W., Li, L., Tong, Z., Kong, X. Oral delivery of insulin using caco 3 -based composite nanocarriers with hyaluronic acid coatings. *Materials Letters*, 188(2017), 263-266.

[50] Yu, W., Jiang, G., Liu, D., Li, L., Tong, Z., Yao, J. Transdermal delivery of insulin with bioceramic composite microneedles fabricated by gelatin and hydroxyapatite. *Materials Science & Engineering C*, 73(2016), 425–428.

[51] Du, X., Jiang, G., Li, L., Yang, W., Chen, H., Liu, Y. Preparation of glucose-sensitive and fluorescence micelles via a combination of photoinitiated polymerization and chemoenzymatic transesterification for the controlled release of insulin. *Journal of Applied Polymer Science*, 133 (2015), 75766-75772.

[52] Jiang, G., Jiang, T., Chen, H., Li, L., Liu, Y., Zhou, H. Preparation of multi-responsive micelles for controlled release of insulin. *Colloid and Polymer Science*, 293 (2015), 209-215.

GRAPHICAL ABSTRACT



Graphic abstract: Schematic representation of nanoparticles

Highlights

1. A comprehensive study of p(AAPBA-b-OVZG) nanoparticles may also help to inspire future designs of insulin or other hypoglycemic protein delivery.
2. p(AAPBA-b-OVZG) is convenient to carry out.
3. p(AAPBA-b-OVZG) is low toxic and safe.
4. The insulin-loaded p(AAPBA-b-OVZG) NPs have a consistent hypoglycemic effect on the mice at least 96 hours.